

---

# Frameless Stereotaxy for Pre-treatment Planning and Post-treatment Evaluation of Radiosurgery

M.L. Schwartz, R. Ramani, P.F. O'Brien, C.S. Young, P. Davey and P. Hudoba

---

**Abstract:** In our centre, 111 patients have been treated with linear accelerator stereotactic radiosurgery. Angiographic, CT and MRI images are generated and the target coordinates calculated in 3 dimensions. For CT scanning, cross sections of perpendicular and oblique fiducial markers are seen. For follow-up CT scans done without the frame, a virtual frame is generated by means of a computer program that places fiducial markers on each CT scan cut, as if the patient had been wearing the OBT frame and the scan produced with the gantry parallel to the base of the frame. The position of the oblique marker may be calculated by knowing the thickness and position of each CT cut. Various natural fiducial markers (bony landmarks) are identified by coordinates in the scan with the patient wearing the real frame and in the scan with the virtual frame applied. A transformation matrix is utilized to establish the equivalence between the original CT scan with the real frame applied and subsequent scans without the real frame but with the virtual frame applied. In effect, the virtual frame is re-applied in exactly the same position as the real frame. Lesion measurements may then be duplicated and growth or regression accurately established. The uncertainty in this system of re-application resides in possible patient movement, CT scan slice thickness and inter-observer error in the identification of natural fiducial markers.

**Résumé:** Stéréotaxie sans cadrage dans la planification avant traitement et l'évaluation après traitement de la radiochirurgie. Cent onze patients ont été traités dans notre centre par radiochirurgie stéréotaxique au moyen d'un accélérateur linéaire. Les images angiographiques, tomодensitométriques et centre par résonance magnétique nucléaire sont générées et les coordonnées de la cible sont calculés en trois dimensions. Pour la tomодensitométrie, des coupes des marqueurs fiduciels en perpendiculaire et en oblique sont visualisées. Pour la tomодensitométrie faite sans cadrage au cours du suivi, un cadrage virtuel est généré au moyen d'un programme informatique qui place les marqueurs fiduciels sur chaque coupe, comme si le patient avait porté le cadrage OBT et le scan est produit avec le pont roulant en position parallèle à la base du cadrage. La position du marqueur oblique peut être calculée en connaissant l'épaisseur et la position de chaque coupe. Différents marqueurs fiduciels naturels (points de repère osseux) sont identifiés par des coordonnées sur le scan alors que le patient porte le vrai cadrage et sur le scan alors que le cadrage virtuel est appliqué. Une transformation matricielle est utilisée pour établir l'équivalence entre le scan original fait avec le cadrage réel et les scans subséquents faits avec le cadrage virtuel, sans le cadrage réel. En fait, le cadrage virtuel est appliqué exactement dans la même position que le cadrage réel. Les mesures de lésions peuvent alors être reproduites et on peut évaluer exactement la progression ou la régression. L'incertitude de ce système est liée à la possibilité que le patient se déplace, à l'épaisseur des coupes et à l'erreur interobservateur dans l'identification des marqueurs fiduciels naturels.

Can. J. Neurol. Sci. 1994; 21: 319-324

---

In our centre, 111 patients; 67 arteriovenous malformations, 34 malignant tumors and 10 acoustic schwannomas, have so far been treated with stereotactic radiosurgery by means of a modified linear accelerator. We have implemented and modified the system originally developed at McGill University.<sup>1,2</sup> The OBT stereotactic head frame<sup>3</sup> and the McGill dynamic rotation method<sup>1</sup> are used. We began with software commercially available from CMI,<sup>4,5</sup> a version of which is also written for the Leksell stereotactic frame, but have made extensive modifications to the software.

The software, which runs on a personal computer, permits the integration of various imaging modalities, digital subtraction

angiography (DSA) computed tomography (CT scanning), and magnetic resonance imaging (MRI).<sup>4,5</sup> It has many functions, allowing the operator to determine the coordinates of any point displayed on a television monitor by positioning the cursor over

---

From the Sunnybrook Health Science Centre (M.L.S.); Toronto Bayview Regional Cancer Centre (R.R., P.F.O., C.S.Y., P.D.); Toronto (Western) Hospital (P.H.), Toronto. RECEIVED FEBRUARY 24, 1994. ACCEPTED IN FINAL FORM JUNE 16, 1994.

Presented in part at the Canadian Congress of Neurological Sciences, Toronto, June 1993.

Reprint requests to: Dr. Michael L. Schwartz, Sunnybrook Health Science Centre, 2075 Bayview Avenue, Suite A129, Toronto, Ontario, Canada M4N 3M5

a structure by means of a mouse. Coronal and sagittal reconstructions may be generated and distances may be measured from one point to another. Additional software, obtained through CMI, but at the time, not otherwise commercially available, allows real three-dimensional dose planning for radiosurgery. This software has been extensively modified by one of the authors (RR) so that treatment plans incorporating as many as four isocentres may be made.

At present, there are only four radiosurgery units in Canada. As a result, we receive angiograms and CT and MR images of patients from centres across the country for consideration of radiosurgical treatment. If one is dealing with a lesion having a complex shape or is considering radiosurgical treatment of a lesion in proximity to radiosensitive structures, for example, the optic chiasm or the brain stem, it is useful to be able to make a treatment plan in advance so that radiation distributions are known and appropriate treatment decisions can be made before the patient travels to our centre. In most cases, our patients return home to be followed by the physicians who referred them. It is essential for us to have an accurate method for following lesion size or determining the geographic location of radiation effect as determined by bright signal on T2-weighted magnetic resonance images to treated lesions.<sup>6</sup>

To these ends, we have developed a method by which a virtual frame is applied to CT or MR images acquired in our centre or elsewhere without the stereotactic frame in place. Once the virtual frame has been applied, all the functions of the software developed for treatment planning may then be used with the CT or MR images acquired without the patient wearing the frame.

**METHODS AND MATERIALS**

The OBT stereotactic frame which is similar to the Leksell stereotactic frame is applied prior to imaging on the day of

radiosurgical treatment and is also used to fix the patient's head to the linear accelerator treatment couch so as to position the patient's lesion at the centre of rotation of both the treatment couch and the linear accelerator gantry which rotate in planes perpendicular to each other. For each imaging modality there is a specific set of fiducial marker plates that attach to the frame. Each CT and MRI fiducial marker plate contains three bars in the shape of an N which, when imaged axially, are seen as three collinear points (Figure 1). Each CT or MR slice contains nine points derived from the three fiducial marker plates. The coordinate corresponding to the third dimension not seen on the individual CT or MRI slices (y) may be calculated by determining the position of the cross-section of the oblique bar of the N. As shown in Figure 1, when transverse slices are obtained parallel to the base of the stereotactic frame, the x and z coordinates of the cross-sections of the vertical bars of the N remain the same in successive transverse CT and MR slices whereas the y coordinate is a function of x and the distance between image slices.

When CT or MRI images made without the patient wearing the stereotactic frame are received for analysis, they are first scanned with a laser digitizer and then converted to the format required by the CMI program by means of software written by one of the authors (RR). These images are transferred to the image directory where they are available to the CMI program so that they then may be viewed on the television monitor. The first (lowest) transaxial image is then assessed and its magnification determined by measuring the five-centimetre scale provided by the CT or MR scanner. The offset distance of each subsequent CT or MRI slice is acquired. In this way, the distance between each cross-section is known. It is assumed that there is no movement of the patient during the acquisition of image slices so that the offset distances indicated by the scanner truly represent the distance between real anatomical features shown slice by slice.

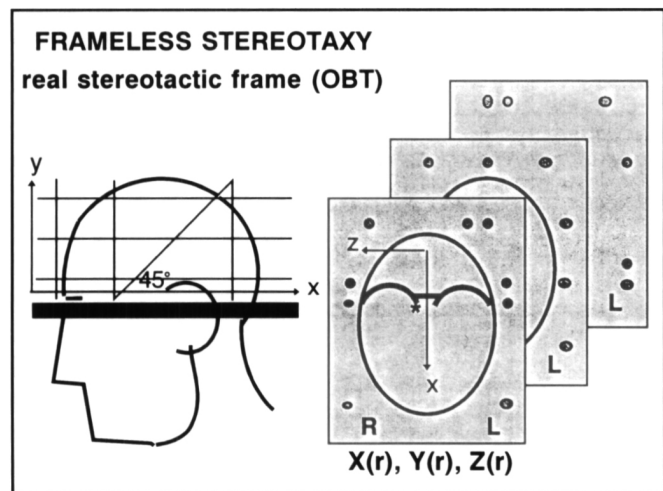


**Figure 1:** Each CT and MRI fiducial marker plate contains 3 bars in the shape of an N, which, when imaged axially, are seen as three collinear points. Each CT or MR slice contains 9 points, derived from the three fiducial marker plates. The coordinate corresponding to the third dimension not seen on the individual CT or MRI slices (y) may be calculated by determining the position of the cross-section of the oblique bar on the N. When transverse slices are obtained parallel to the base of the stereotactic frame, the x and z coordinates of the cross-sections of the vertical bars of the N have the same x and z coordinates as they appear in successive transverse CT and MR slices and y is a function of x and the distance between the image slices.

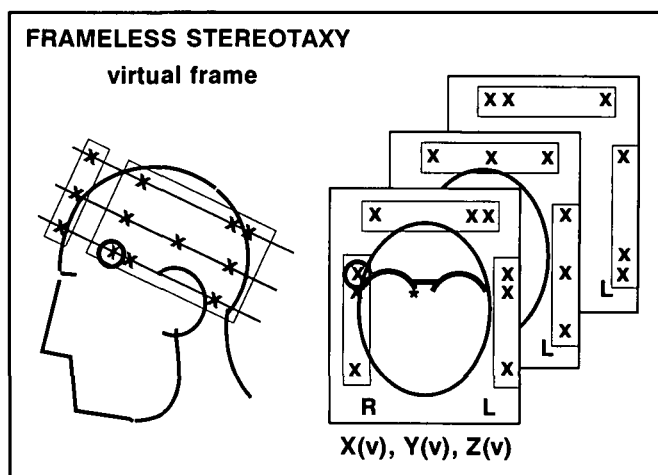


**Figure 2:** A virtual frame is generated with an arbitrary starting point, the cross-section of a vertical marker, as indicated by the circled X. This marker may be placed anywhere and need not be outside the patient's head. The position of the other vertical markers is automatically determined by choosing the starting point because the cross-sectional appearance of the stereotactic frame is known and the scale of the image has been measured. In effect, the other vertical markers are placed as though the scan had been made with the patient wearing a stereotactic frame with the CT or MR image plane parallel to the base of the frame.

A virtual frame is then generated with an arbitrary starting point, such as the cross-section of a vertical marker indicated in Figure 2 by the circled x. This marker may be placed anywhere and need not be outside the patient's head. The position of the other vertical markers is automatically determined by choosing the starting point because the cross-sectional appearance of the stereotactic frame is known and the scale of the image has been measured. In effect, the other vertical markers are placed as though the scan had been made with the patient wearing a stereotactic frame with the CT or MR image plane parallel to the base of the frame. The position of the cross-section of the oblique bar of the N may then also be displayed because the offset of each transverse slice is known. Partial correction for patient movement or malregistration of images digitized by the scanner is achieved by generating a coronal or sagittal reconstruction and manually aligning structures such as the cranial vault known to have a regular contour.

Various natural fiducial markers are then selected. Criteria for choosing anatomical points have been suggested by Hill et al.<sup>9</sup> They propose any point – like structures, (e.g., the apical turn of the cochlea; the intersection of two linear structures, such as blood vessel bifurcations, the intersection of a surface with a linear structure, as where a nerve passes through a foramen or the intersection of three surfaces). In our experience, the anterior clinoid process (as indicated in Figure 3), the apex of the internal auditory canal and the promontory of the inner ear have proved most useful. Since all geometric functions of the CMI software apply, coronal and sagittal reconstructions may be made. The alternate views are helpful to refine the choice of the best locus of the selected natural fiducial marker. Three views of each selected natural fiducial marker are obtained and the best coordinates of the selected point determined using the software and the arbitrarily-placed virtual frame. The coordinates of the selected fiducial marker indicated in Figure 3 are given as  $x(v)$ ,  $y(v)$  and  $z(v)$ .

The same natural fiducial markers are then imaged and their coordinates determined in another CT or MRI scan, done with

the patient actually wearing the OBT frame. The coordinates with the patient wearing the real frame are given as  $x(r)$ ,  $y(r)$  and  $z(r)$  in Figure 3. Because the position of the real frame with respect to the patient's head is different from that of the virtual frame, the coordinates given by the CMI program for a particular landmark are different from those given for the virtual frame applied to the CT or MRI study.

As the real and virtual frames have the same size and shape, the coordinates for any recognizable landmark in one study are related to those of the equivalent point in the other study, as though translation and rotation of the same frame had occurred between studies. As a result, using a transformation matrix and any three equivalent points, the coordinates for any point on the display of any CT or MRI slice, as given by  $x(v)$ ,  $y(v)$  and  $z(v)$ , may be transformed to  $x(t)$ ,  $y(t)$  and  $z(t)$ . Conceptually, the transformation matrix translates and rotates the virtual frame to the same position as the real frame with respect to the patient's head. The error in this system of transformation resides in CT or MRI scan slice thickness, interobserver error in the identification of natural and frame fiducial markers and movement of the patient in the CT or MRI scanner at the time of the study done without the real stereotactic frame. This error has been measured and is described below.

## RESULTS

The effect of slice thickness on the accuracy of the identification of bony landmarks as natural fiducial markers is significant. The first study was done with the patient wearing the stereotactic frame to evacuate a tumor cyst. A second study, done for further patient management without the stereotactic frame in place was produced with 5 millimetre-thick CT scan slices. Care was taken to immobilize the patient's head in the CT scanner so that movement between slices was impossible. Four bony anatomical points easily seen in the studies done with and without the real stereotactic frame were selected and the transformation method applied. No coronal or sagittal reconstructions were used. The distance from anatomical point 1 to point 2 was measured in the CT scan done with frame and then in the study done without. Similarly, distances between points 1 and 3, 1 and 4, 2 and 3, 2 and 4, and between 3 and 4 were determined. The CT scan, done with the stereotactic frame in place, was taken as the "gold standard". The differences in these measurements between the study with frame and the frameless study were considered to be the measurement errors. These are shown in Table 1. The measurement errors were determined and the contributions of the  $x$ ,  $y$  and  $z$  error vectors to the total error were determined. The standard deviations were  $x = 2.8$  mm,  $y = 5.53$  mm and  $z = 2.23$  millimetres.

As part of a protocol to measure the change in apparent size of cerebral metastases after a delay following the injection of iodinated contrast material, two separate CT scans utilizing 1 mm slices were made 40 minutes apart with a patient wearing the stereotactic frame. The co-ordinates of four bony anatomical landmarks are indicated in Table 2. The first study was made with the CT gantry (image plane) parallel to the base of the OBT frame and the second with the frame deliberately placed at an angle to the CT image plane. The coordinates of the natural fiducial markers (anatomical landmarks) with respect to the stereotactic frame which had not moved relative to the patient's

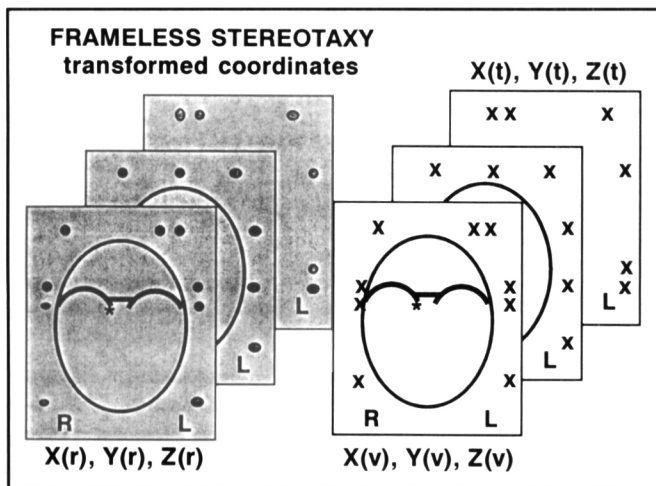


**Figure 3:** The anterior clinoid process, as indicated by the asterisk may be chosen as a natural fiducial marker. Three views of each selected natural fiducial marker are obtained. The coordinates of equivalent points identified in the real and virtual frames are designated (r) and (v) respectively. Transformed coordinates (t) may be compared with  $x(r)$ ,  $y(r)$ ,  $z(r)$ .

**Table 1.** Four easily identifiable bony anatomical points were selected. Column one indicates which distances were measured. Columns two and three give the interpoint distances with the real and virtual frames respectively.

Error estimates in frameless stereotaxy		
Points	Real Frame	Virtual Frame: Transformed Coordinates
1 – 2	43.5	42.9
1 – 3	61.7	62.1
1 – 4	57.6	52.4
2 – 3	30.5	31.3
2 – 4	55	51.8
3 – 4	45.1	46.8

SD x = 2.8 mm    y = 5.53 mm    z = 2.23 mm

head would be expected to be the same in both studies although the appearance of the CT slices was quite different because of change in the position of the patient's head (and stereotactic frame) with respect to the CT scan image plane. Any difference in coordinates in one study from those of the same point in another study represents the error in identifying the same bony landmark in different CT scans. It was impossible to reliably identify the same point on the promontory of the inner ear in the two studies because of the different CT angle but the centre of the clinoid process and the apex of the internal auditory meatus proved resistant to translation and rotation with respect to the CT image plane. The error attributable to the uncertainty in identifying the anatomical landmarks was (standard deviations)  $x = 0.43$  mm,  $y = 0.71$  mm and  $z = 0.43$  mm. The computation error, that is, the residual error after subtracting the anatomical landmark error was negligible. The pixel size of our display system (software and hardware) is 0.67 millimetres.

Figure 4 shows a sagittal reconstruction through the right anterior clinoid process in a patient with an acoustic neuroma.

The cursor has been placed at the mid-point of the anterior clinoid process in its vertical dimension. Utilization of the coronal or sagittal reconstructions allows the observer to choose the locus of a bony landmark more reliably than if the reconstructions were not available.

Figure 5(a) shows a malignant astrocytoma, recurrent after partial surgical resection and conventional fractionated external beam photon irradiation. The patient was referred for consideration of palliative treatment using conformal radiosurgery. As the tumor is close to the optic nerve and as the development of a treatment plan with several isocentres may be complex and time-consuming, the virtual frame was applied to the CT scan done at another hospital and the radiation isodose contours indicated in Figure 5(a) was produced. It was elected to treat the patient. The actual treatment plan utilized is indicated in Figure 5(b). None of the nine coordinates specifying the three treatment isocentres had to be changed by more than two millimetres in converting the treatment plan derived from the CT scan done at another hospital without the stereotactic frame to the treatment plan actually used.

## DISCUSSION

Frameless methods have been developed for stereotactic radiosurgery, but all require some method of reliably positioning the patient with respect to the radiation source. Jones and his colleagues<sup>7</sup> have used gold markers implanted in the skin and a moulded semi-rigid face mask to help hold the patient in place during treatment. The gold markers have the virtue of being visible on plain radiographs, permitting their identification on beam films. They emphasize that patient co-operation in lying still during treatment is essential. Phillips et al.<sup>8</sup> also use a face-mask with markers to obviate the stereotactic frame during treatment but comment that the errors in repositioning the mask "are on the order of several millimetres". Since any method of positioning a patient for radiosurgery without a frame must

**Table 2.** The anatomical landmarks chosen are shown in column one. The differences in co-ordinates between columns two and three represent the error in identifying the same bony anatomical landmark in two different CT images produced at different angles. Column four gives the co-ordinates produced by the arbitrarily applied virtual frame. The differences between column five and one are the sum of the point identification error and the computational error.

Error estimates in frameless stereotaxy				
Anatomical Point	Coordinates with Real Frame: 1	Coordinates with Real Frame: 2	Coordinates with Virtual Frame	Transformed Coordinates
Right Internal Auditory Canal	8.5, 3.3, 4.2	8.5, 3.3, 4.3	7.7, 5.1, 2.9	8.3, 3.2, 4.1
Left Internal Auditory Canal	8.8, 3.5, -3.4	8.9, 3.6, -3.3	7.6, 4.7, -4.5	8.8, 3.5, -3.4
Right Anterior Clinoid Process	4.8, 3.8, 1.7	5.0, 4.0, 1.8	4.3, 6.1, 0.9	5.0, 3.9, 1.8
Left Anterior Clinoid Process	5.1, 3.8, -1.3	5.1, 3.9, -1.3	4.0, 5.7, -2.2	4.9, 3.8, -1.3

SD x = 0.43 mm    y = 0.71 mm    z = 0.43 mm

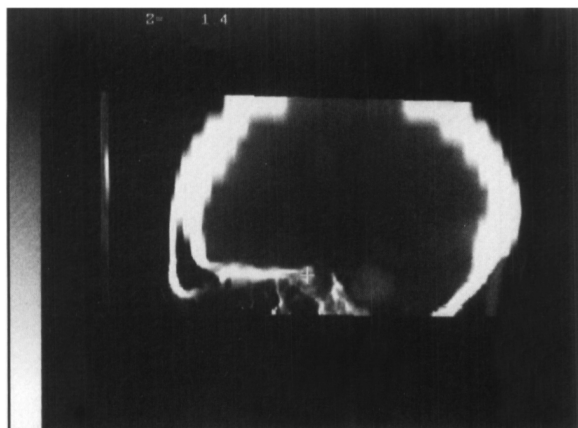


**Figure 4:** The cursor has been placed at the midpoint of the anterior clinoid process as seen in the sagittal reconstruction through the right anterior clinoid process in a patient with an acoustic neuroma. Utilization of the coronal or sagittal reconstructions allows the observer to choose the locus of a bony landmark more reliably than if the reconstructions were not available.

provide precise, accurate localization that does not change during treatment, it may be that so-called frameless methods will require attachments that in effect will constitute a re-locatable frame. In our centre, we have not yet devised a method of positioning the patient for radiosurgery without the stereotactic frame.

The use of anatomical features as fiducial markers has been used by Hill et al.<sup>9</sup> for the integration of information derived from MRI and CT scanning for use in surgical planning. They also select equivalent recognizable points in two studies that they wish to combine. These landmarks are utilized to get the two images in register by means of an algorithm that translates and rotates one image so that equivalent points correspond. As a last step, bone densities obtained from CT scanning are combined with soft tissue densities obtained from MRI scanning. Composite transaxial images are then produced. The accuracy is to within 1.5 millimetres. The disadvantage of the system is that it requires two SUN work stations whereas our system is a single personal computer with an Intel 486 microchip running DOS 5.0 (copyright Microsoft Corporation). The production of fused images has not been implemented because it exceeds the practical limits of our system. As an alternate strategy, the planning software has recently been further modified to run under Windows (copyright Microsoft Corporation). Equivalent anatomical points may be identified in different studies by their stereotactic coordinates and the image in view changed instantly from one to another by a single keystroke, thus permitting the integration of information from different imaging modalities for treatment planning and follow-up.

#### CONCLUSION

The error due to uncertainty in finding the same bony landmarks (natural fiducial markers) in different CT studies depends in part on slice thickness and is as little as 0.43 in 1 mm slices. The computational error is negligible. The potential error caused by patient movement between slices cannot be quantified but may be recognized and partially compensated for. This method

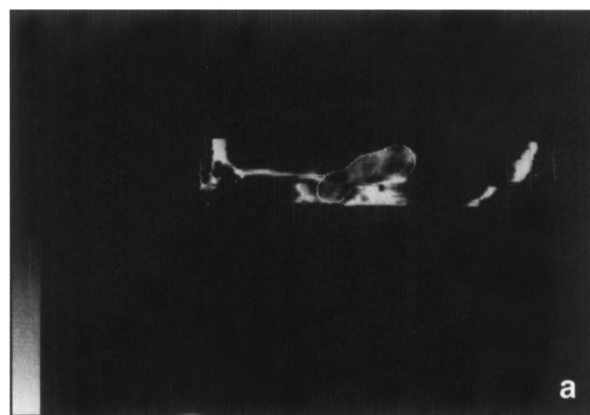


**Figure 5(a):** The sagittal reconstruction of a CT scan done at another hospital without a stereotactic frame in place is illustrated. The lateral reconstruction has a flattened appearance as compared with image in Figure 8 but equivalent structures have equivalent co-ordinates. A treatment plan with 3 isocentres was made by applying the virtual frame to the CT scan and using the radiosurgery planning software.

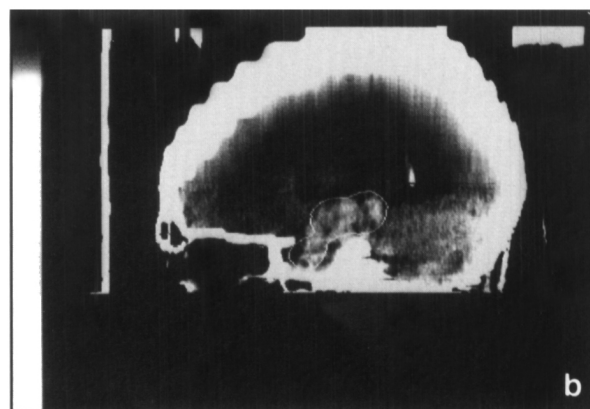


**Figure 5(b):** The actual treatment plan used for this patient produced with him wearing the real stereotactic frame is illustrated. None of the 9 coordinates specifying the 3 treatment isocentres had to be changed by more than 2 millimetres.

of frameless stereotaxy has proved useful in radiosurgical planning and follow-up. Its use for treatment in our centre awaits further development.

#### REFERENCES

1. Podgorsak EB, Olivier A, Pla M, et al. Dynamic stereotactic radiosurgery. *Int J Radiat Oncol Biol Phys* 1988; 14: 115-125.
2. O'Brien PF, Gillies BA, Schwartz ML, et al. Radiosurgery with unflattened 6-MV photon beams. *Med Phys* 1991; 18(3): 519-521.
3. Olivier A, Bertrand G. Stereotaxic device for percutaneous twist-drill insertion of depth electrodes and for brain biopsy. *J Neurosurg* 1982; 56: 307-308.
4. Peters TM, Clark JA, Olivier A, et al. Integrated stereotaxic imaging with CT, MR imaging, and digital subtraction angiography. *Radiology* 1986; 161(3): 821-826.
5. Henri CJ, Collins DL, Peters TM. Multimodality image integration for stereotactic surgical planning. *Med Phys* 1991; 18(2): 167-177.

6. Kauczor HU, Engenhardt R, Layer G, et al. 3D TOF MR angiography of cerebral arteriovenous malformations after radiosurgery. *Comput Assist Tomogr* 1993; 17(2): 184-190.
7. Jones D, Christopherson DA, Washington JT, et al. A frameless method for stereotactic radiotherapy. *Br J Radiol* 1993; 66: 1142-1150.
8. Phillips MH, Kessler M, Chuang FYS, et al. Image correlation of MRI and CT in treatment planning for radiosurgery of intracranial vascular malformations. *Int J Radiat Oncol Biol Phys* 1991; 20: 881-889.
9. Hill DLG, Hawkes DJ, Crossman JE, et al. Registration of MR and CT images for skull base surgery using point-like anatomical features. *Br J Radiol* 1991; 64: 1030-1035.